Alkali Metal-Templated Assembly of Cyanometalate "Boxes" $(NEt_4)_3\{M[Cp^*Rh(CN)_3]_4[Mo(CO)_3]_4\}$ (M = K, Cs). Selective Binding of Cs^+

Kevin K. Klausmeyer, Scott R. Wilson, and Thomas B. Rauchfuss*

Contribution from the School of Chemical Sciences and the Frederick Seitz Materials Research Laboratory, University of Illinois at Urbana-Champaign, Urbana, Illinois 61801

Received July 6, 1998

Abstract: The box-like cages $\{M[Cp^*Rh(CN)_3]_4[Mo(CO)_3]_4\}^{3-}$ form as the sole metal-containing products of the reaction of $[Cp^*Rh(CN)_3]^-$ and $(\eta^6\text{-}C_6H_3Me_3)Mo(CO)_3$ in the presence of K^+ and Cs^+. Well-defined species could not be identified in solutions of $Cp^*Rh(CN)_3^-$ and $(\eta^6\text{-}C_6H_3Me_3)Mo(CO)_3$ in the absence of alkali metal cations. The new cages were isolated as their Et_4N^+ salts, M = K^+ (**1**), Cs^+ (**2**). Crystallographic characterization of **1** and **2** reveals box-like $M_8(\mu\text{-}CN)_{12}$ cages containing alkali metal cations. The cages feature 12 external CO and 4 external C_5Me_5 ligands. In **1**, the K^+ is disordered over two off-center positions, whereas in the case of **2**, the Cs^+ is centered in the cage with a formal coordination number of 24. Otherwise, the structures of the two compounds are virtually indistinguishable. The persistence of the solid-state structures in solution was established through ^{13}C NMR spectroscopy and electrospray mass spectrometric measurements. ^{133}Cs NMR spectroscopy, which readily distinguishes free from included Cs^+, shows that the boxes preferentially bind Cs^+ relative to K^+.

Introduction

Alkali metal binding to inorganic frameworks,[1] e.g., zeolites and clays, is not only technically interesting but is also useful. For example, ion exchange by zeolites is used for water softening, the removal of radionuclides,[2] and the modification of the catalytic properties.[3] Relative to traditional organic complexants such as polyamines and polyethers, inorganic ion-exchange materials are often more selective due to their rigidity.[4,5] In contrast, flexible organic ligands tend to favor small ions with large charge/radius ratios. It is true, however, that through ingenious synthesis, organic ligands have been prepared that preferentially bind to larger alkali metals.[6−9] The ability of rigid ligands to confer selectivity is illustrated by the behavior of the inorganic inclusion complex $[NaAu_{12}Se_8]^{3-}$, which is synthesized by the hydrothermal reaction of Au and Na_xSe_2.[10] The K^+ analogue of this complex cannot be prepared because the larger K^+ (r_{K^+} = 1.38 Å vs r_{Na^+} = 1.02 Å) is incompatible with the cavity in the $Au_{12}Se_8$ cage.

The cyanometalates,[11,12] such as Prussian blue,[13] are coordination polymers that are well-known to exhibit ion-exchange properties. Ion exchange in these materials is facilitated by the relatively large $M_4(CN)_4$ windows (∼25 Å^2), which allow transport of guest ions into the cavities.[14] In some cases it is clear that the alkali metals occupy the interior of the cubic $M_8(CN)_{12}$ box-like cages. As related by Dunbar[11] and more recently Davis,[9] Prussian blue analogues are of interest as sequestering agents for Cs^+. Cs-selectivity is of interest[15−19] because ^{137}Cs is a dangerous radionuclide ($t_{1/2}$ = 30 y, β^- emission) that is a major product of uranium and plutonium fission. In fact, cyanometalates have been administered orally in cases of acute $^{137}Cs^+$ poisoning.[11] In this paper, we describe a soluble cubic cyanometalate framework that, like the solid-state materials, binds alkali metal cations with a particular affinity for Cs^+.

The present contribution extends our recent synthesis of "molecular boxes," cages consisting of metals situated at the corners of a cube, all linked by CN bridges.[20] The connectivity of these species can be understood by considering the synthesis

(1) Wells, A. F. *Structural Inorganic Chemistry*, 5th ed.; Clarendon Press: Oxford, 1984.
(2) Chen, N. Y.; Degnan, T. F.; Smith, C. M. *Molecular Transport and Reaction in Zeolites*; VCH: New York, 1994.
(3) Gates, B. C. *Catalytic Chemistry*; John Wiley & Sons: New York, 1992.
(4) Scharff, J. P.; Mahjoubi, M.; Perrin, R. *New. J. Chem.* **1991**, *15*, 883.
(5) Izatt, R. M.; Pawlak, K.; Bradshaw, J. S.; Bruening, R. L. *Chem. Rev.* **1995**, *95*, 2529.
(6) Bradshaw, J. S.; Izatt, R. M. *Acc. Chem. Res.* **1997**, *30*, 338.
(7) Krakowiak, K. E.; Bradshaw, J. S.; Zhu, C.; Hathaway, J. K.; Dalley, N. K.; Izatt, R. M. *J. Org. Chem.* **1994**, *59*, 4082.
(8) Assmus, R.; Böhmer, V.; Harrowfield, J. M.; Ogden, M. I.; Richmond, W. R.; Skelton, B. W.; White, A. H. *J. Chem. Soc., Dalton Trans.* **1993**, 2427.
(9) Davis, J. T.; Tirumala, S. K.; Marlow, A. L. *J. Am. Chem. Soc.* **1997**, *119*, 5271.
(10) Huang, S.-P.; Kanatzidis, M. G. *Angew. Chem., Int. Ed. Engl.* **1992**, *31*, 787.
(11) Dunbar, K. R.; Heitz, R. A. *Prog. Inorg. Chem.* **1997**, *45*, 283.
(12) Sharpe, A. G. *The Chemistry of Cyano Complexes of the Transition Metals*; Academic Press: London, 1976.
(13) Herren, F.; Fischer, P.; Ludi, A.; Hälg, W. *Inorg. Chem.* **1980**, *19*, 956.
(14) Brousseau, L. C.; Williams, D.; Kouvetakis, J.; O'Keeffe, M. *J. Am. Chem. Soc.* **1997**, *119*, 6292.
(15) Davis, B. M.; Serba, F. *J. Appl. Chem.* **1967**, *17*, 40.
(16) Kouřím, V.; Rais, J.; Million, B. *J. Inorg. Nucl. Chem.* **1964**, *26*, 1111.
(17) Prout, W. E.; Russell, E. R.; Groh, H. J. *J. Inorg. Nucl. Chem.* **1965**, *27*, 473.
(18) Vlasselaer, S.; D'Olieslager, W.; D'Hont, M. *J. Inorg. Nucl. Chem.* **1976**, *38*, 327.
(19) Schulz, W. W.; Bray, L. A. *Sep. Sci. Technol.* **1987**, *22*, 191.
(20) Klausmeyer, K. K.; Wilson, S. R.; Rauchfuss, T. B. *Angew. Chem., Int. Ed. Engl.* **1998**, *110*, 1808.

10.1021/ja982347w CCC: $18.00
Published on Web 03/12/1999

of the box $\{[CpCo(\mu\text{-}CN)_3]_4[Cp^*Rh]_4\}^{4+}$, by the coupling of $[CpCo(\mu\text{-}CN)_2(CN)]_2[Cp^*RhCl]_2$ (the eight-component reaction of $[CpCo(CN)_3]^-$ and $[Cp^*Rh(MeCN)_3]^{2+}$ works as well, eq 1). The M−CN linkages, which remain intact throughout the

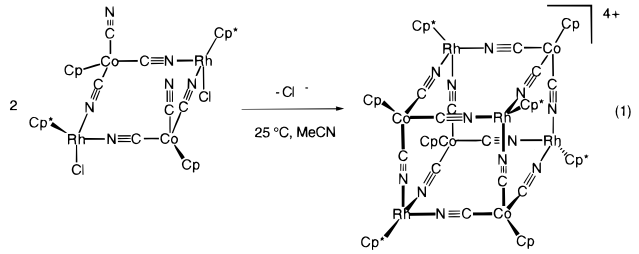

(1)

assembly process, displace labile MeCN ligands. In related work, Long and co-workers have employed triazacyclononane (TACN) as face-capping ligands in the assembly of related but more highly cationic cages.[21]

Given their considerable interior volume (~135 Å^3), as well as the aforementioned precedents in the chemistry of solid cyanometalates, the $M_8(CN)_{12}$ cages have the potential to exhibit inclusion properties. Initial indications of cation binding in these molecular boxes came from an attempted preparation of the charge-neutral species $[CpCo(\mu\text{-}CN)_3]_4[Cp^*Ru]_4$. The mass spectrum of the soluble products of this reaction gave peaks corresponding to $K[CpCo(CN)_3]_4[Cp^*Ru]_4^+$ (eq 2).[22] We ten-

$$4\ CpCo(CN)_3^- + 4\ Cp^*Ru(MeCN)_3^+ \xrightarrow[-12MeCN]{K^+} \{K[CpCo(CN)_3]_4[Cp^*Ru]_4\}^+ \quad (2)$$

tatively interpreted this result as indicating the formation of a cage with K^+ at its interior. Rationalizing that alkali metal cations would bind still more strongly to *anionic* cages, we turned to the preparation of cages derived from $[Cp^*Rh(CN)_3]^-$ and $(\eta^6\text{-}C_6H_3Me_3)Mo(CO)_3$, a source of the $Mo(CO)_3$ fragment.[23,24]

Results

Synthesis and Spectroscopic Characterization. The reaction of $(Et_4N)[Cp^*Rh(CN)_3]$ and $(\eta^6\text{-}C_6H_3Me_3)Mo(CO)_3$ was found to proceed at room temperature in minutes. Complete displacement of mesitylene was indicated by ^{1}H NMR analysis; the resulting solutions were stable, provided that they are protected from the atmosphere. Because the arene is displaced, we conclude that the Mo centers achieve 6-coordination via complexation to the N termini of the coordinated CN ligands as well as to the solvent MeCN. ^{1}H NMR measurements indicate that the reaction mixture consists of one principal Cp*-containing species (~ 75%), but other species are evident including $Cp^*Rh(CN)_3^-$ (δ 1.86, see Figure 1). Similarly, ^{13}C NMR analysis showed a complex mixture of Cp*Rh-containing species including $Cp^*Rh(CN)_3^-$.

A low yield of well-formed crystals could be obtained by addition of Et_2O to the reaction mixture described above. The crystals proved to consist of $(NEt_4)_3\{K[Cp^*Rh(\mu\text{-}CN)_3]_4[Mo(CO)_3]_4\}$ (**1**), together with various molecules of solvation (vide infra). The low yield can be attributed to the fact that the K^+, which is required for crystal growth, was present as a trace

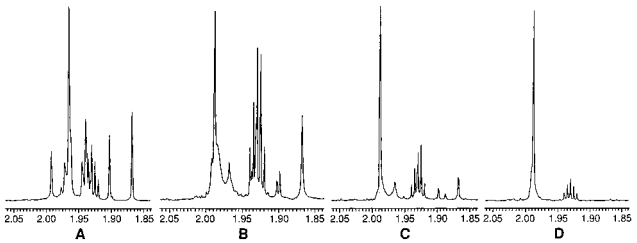

Figure 1. 500 MHz ^{1}H NMR measurements showing the influence of CsOTf on the reaction $(Et_4N)[Cp^*Rh(CN)_3] + (\eta^6\text{-}C_6H_3Me_3)Mo(CO)_3$. Spectrum A is that of a stock MeCN solution that is equimolar in the two metal complexes (this spectrum remains unchanged over 72 h). Spectrum B is the same stock solution 20 min after it was treated with 0.25 equiv CsOTf. Spectrum C is the same solution (i.e., that used for spectrum B) after 48 h. Note the simplification of the Cp* region. For spectrum D, the sample was prepared by adding MeCN to a solid mixture of $(Et_4N)[Cp^*Rh(CN)_3]$, $(\eta^6\text{-}C_6H_3Me_3)Mo(CO)_3$, and 1 equiv CsOTf in a 4:4:1 molar ratio after 24 h. The signal at δ 1.86 is due to $Cp^*Rh(CN)_3^-$.

impurity in the starting $(Et_4N)[Cp^*Rh(CN)_3]$ (prepared by reaction of KCN and $[Cp^*RhCl_2]_2$, followed by cation exchange with Et_4NCl). The fact that **1** formed in the presence of low concentrations of K^+ indicates that the cyanometalate cage has a high affinity for the alkali metal cation. Subsequent ^{1}H NMR measurements showed that **1** forms efficiently when the reaction of $(Et_4N)[Cp^*Rh(CN)_3]$ and $(\eta^6\text{-}C_6H_3Me_3)Mo(CO)_3$ is conducted in the presence of 0.25 equiv of $KB(C_6H_4\text{-}4\text{-}Cl)_4$, a MeCN-soluble source of K^+. Similarly, we obtained a related Cs^+-containing product **2** when the reaction was conducted in the presence of CsOTf (eq 3). These salts were purified by

$$4\ Cp^*Rh(CN)_3^- + 4\ (C_6H_3Me_3)Mo(CO)_3 \xrightarrow[-\ 4\ C_6H_3Me_3]{+\ K^+\ or\ Cs^+} \{M[Cp^*Rh(CN)_3]_4[Mo(CO)_3]_4\}^{3-} \quad (3)$$
$$M = K^+(\mathbf{1}),\ M = Cs^+(\mathbf{2})$$

fractional crystallization from MeCN−Et_2O solutions to remove the coproduct $(Et_4N)OTf$.

The new compounds were obtained as crystals that proved extremely sensitive to desolvation. Air-drying of these samples afforded solvent-free materials that were subjected to microanalysis. In the case of **2**, vacuum-dried, desolvated samples gave good results upon conventional combustion analysis. We were unable to obtain high quality combustion analytical results for **1**; this finding is consistent with the fact that even recrystallized samples contain some $Cp^*Rh(CN)_3^-$, as indicated by ^{1}H and ^{13}C NMR analysis. We interpret these findings as indicating that **1** is slightly labile with respect to loss of K^+, in accord with the relative stability of the Cs^+ vs K^+ derivatives (vide infra). Both **1** and **2** were also analyzed for their metal content by electron microprobe analysis (EDX). This technique, which has precision of ±5%, established that the metal ratios corresponded to MRh_4Mo_4, for M = K, Cs. Additionally, the EDX technique allowed us to establish the homogeneity of the new materials through the analysis of several parts of a given sample on a electron microscope stage.

Electrospray mass spectrometric (ESI-MS) measurements show that these molecular cages exist in solution. Spectra of MeCN solutions of **1** and **2** showed peak envelopes for the ion pair $\{(Et_4N)K[Cp^*Rh(\mu\text{-}CN)_3]_4[Mo(CO)_3]_4\}^{2-}$ (m/z = 1077.6) and the parent cluster $\{Cs[Cp^*Rh(\mu\text{-}CN)_3]_4[Mo(CO)_3]_4\}^{3-}$ (m/z = 705.8), respectively. The mass distribution of molecular ion peak envelope matched that calculated from the isotopic abundances. The ESI-MS of all samples, including those lacking

(21) Heinrich, J. L.; Berseth, P. A.; Long, J. R. *Chem. Commun.* **1998**, 1231.
(22) Contakes, S. M. unpublished results.
(23) Pidcock, A.; Smith, J. D.; Taylor, B. W. *J. Chem. Soc.* **1967**, 872.
(24) Zingales, F.; Chiesa, A.; Basolo, F. *J. Am. Chem. Soc.* **1966**, *88*, 2707.

in alkali metal cations, showed intense peaks for $[Cp^*Rh(CN)_3]^-$ and $Cp^*Rh(CN)_3[Mo(CO)_3]^-$ (the latter is not the octametallic tetraanion as judged by the *m*/*z* spacing) The nature of the latter species is not known; one speculative suggestion is that the binding of the $Mo(CO)_3$ unit to the $Cp^*Rh(CN)_3^-$ moiety resembles the binding of Na^+ to $CpFe(CN)_2(CO)^-$.[25]

NMR measurements proved very useful in assessing the purity, structure, and stability of the new cyanometalate cages. ^{1}H NMR measurements on MeCN solutions readily distinguish the predominant species formed in the absence of alkali metals (δ 1.966) from **1** (δ 1.994) and **2** (δ 1.988). In the case of **2**, the same cage species is formed regardless of the order of mixing, thus the components of the mixture equilibrate readily. ^{1}H NMR measurements also allowed us to verify the integrity of solutions of **2** prepared from desolvated samples used for microanalysis. The only difference between the ^{1}H NMR spectra of these purified samples and crude reaction solutions of **2** was the Cp^*/Et_4N^+ ratio. The ^{13}C NMR spectrum of **2**-$(^{13}C)_{12}$ consists of a doublet in the CN region (δ 129.1, $J = 51$ Hz), similar to that seen for $\{[CpCo(\mu\text{-}CN)_3]_4[Cp^*Rh]_4\}^{4+}$ (δ 132.4, no $^{13}C\cdots^{103}Rh$ coupling because the Co is bound to the carbon of CN) and $(Et_4N)[Cp^*Rh(CN)_3]$ (δ 128.9, $J = 51$ Hz). The doublet splitting, due to ^{103}Rh coupling, confirms the integrity of the Rh−CN linkages.

The IR spectra of the cyanometalate cages confirmed the connectivity (terminal vs bridging) of the CN ligands. Solutions of $(Et_4N)[Cp^*Rh(CN)_3]$ (in MeCN or CH_2Cl_2) show IR bands at 2120 and 2114 cm^{-1}; the presence of two bands is consistent with the C_{3v} geometry, while the band positions indicate terminal CN ligands. IR spectra of **1** and **2** differ from that for $Cp^*Rh(CN)_3^-$ as only a single ν_{CN} band is observed at 2147 cm^{-1}, consistent with μ-CN groups. A signal at 2147 cm^{-1} also dominates the spectrum for a MeCN solution equimolar in $(Et_4N)[Cp^*Rh(CN)_3]$ and $(\eta^6\text{-}C_6H_3Me_3)Mo(CO)_3$ (but lacking M^+). It appears that CN is bridging in the alkali metal-free case, although the ^{1}H and ^{13}C NMR data, as well as the ESI-MS results (vide supra), argue against box formation.

Under idealized T_d symmetry assumed for **1** and **2**, the basis set of 12 μ-CN ligands gives rise for five normal vibrational modes of A_1, E, T_1, and T_2 (2) symmetry. The two T_2 modes are IR active. While we do not observe two bands for **1** and **2**, the 2147 cm^{-1} band is broad. Furthermore, the previously reported $\{[CpCo(\mu\text{-}CN)_3]_4[Cp^*Rh]_4\}^{4+}$ also exhibits only one broad ν_{CN} band.[20] A single ν_{CN} band was also reported for the cubic solid-state polymers $[M(CN)_3]_n$ (M = Ga, In) (2200−2215 cm^{-1}),[26] and the molecular boxes reported by Long et al. $[(TACN)Co]_8(\mu\text{-}CN)_{12}[OTf]_{12}$ (2200 cm^{-1}) and $[(TACN)Co(\mu\text{-}CN)_3]_4[(TACN)Cr]_4[OTs]_{12}$ (2177 cm^{-1}).[21]

A two-band ν_{CO} pattern is observed for both **1** and **2**, consistent with *fac*-$M(CO)_3$ subunits.

Crystallographic Characterization of $(Et_4N)_3\{M[Cp^*Rh(\mu\text{-}CN)_3]_4[Mo(CO)_3]_4\}$ (M^+ = Cs, K). Both **1** and **2** readily crystallize as yellow-orange blocks upon diffusion of Et_2O into MeCN solutions of these compounds. The compounds are isostructural as indicated by very similar values for the cell constants; this was expected because the packing in the crystal should be unaffected by the contents of the cage. Due to their similarities, the structures of **1** and **2** will be discussed together. As indicated by the internal consistency parameter, R_{int}, the reflection data for **1** are better than that for **2**.

The box-like cages are highly regular (see Figure 2); the Rh−C−N and Mo−N−C links are 180 ± 11°. Similarly the (N)C−Rh−C(N) and (C)N−Mo−N(C) angles are ∼90 ± 10°. The Mo−N distances range from 2.2 to 2.241 Å. Comparable distances of ∼2.23 Å are seen in other nitrile adducts, e.g., $Mo_2(SPh)_2(CO)_6(NCMe)_2$,[27] although the compounds $Mo(CO)_{6-n}(NCR)_n$ have not been crystallographically characterized. Exterior to the $Mo_4Rh_4(CN)_{12}$ core are 12 terminal CO and 4 Cp* groups. The CO ligands are linear, and the C−O distances are unremarkable.

The Mo_4Rh_4 cores in **1** and **2** are virtually indistinguishable and are highly symmetrical. Across the faces of the cage, the Rh···Rh and Mo···Mo distances are 7.38 and 7.72 Å, respectively for both **1** and **2** (see Tables 1 and 2). In $\{[CpCo(\mu\text{-}CN)_3]_4[Cp^*Rh]_4\}^{4+}$, the Rh···Rh distance was 7.3676(1) Å. The body diagonal distance, e.g., for Mo1−Rh4, is 9.25 Å; the

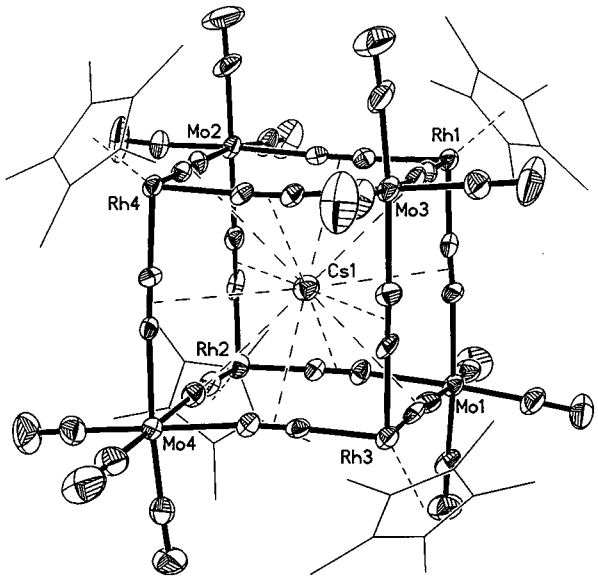

Figure 2. SHELXTL plot of $\{Cs[Cp^*Rh(\mu\text{-}CN)_3]_4[Mo(CO)_3]_4\}^{3-}$ (35% probability ellipsoids except for Cp* groups).

Table 1. Selected Structural Features (Å) for the $\{K[Rh(\mu\text{-}CN)_3]_4Mo_4\}^{3-}$ Core in **1**

5.3570 (0.0007)	Rh1−Mo1	7.3613 (0.0006)	Rh1−Rh4
5.3497 (0.0007)	Rh1−Mo2	7.7251 (0.0007)	Mo1−Mo2
5.3695 (0.0007)	Rh1−Mo3	7.7102 (0.0006)	Mo1−Mo3
9.2484 (0.0007)	Rh1−Mo4	7.7218 (0.0007)	Mo1−Mo4
7.3886 (0.0006)	Rh1−Rh2	9.2511 (0.0006)	Mo1−Rh4
7.3922 (0.0007)	Rh1−Rh3		
7.1125 (0.0075)	C1−C12	7.1190 (0.0069)	N1−N12
7.4277 (0.0082)	C2−C9	7.4351 (0.0070)	N2−N9
7.4852 (0.0075)	C3−C6	7.6279 (0.0067)	N3−N6
7.4903 (0.0075)	C4−C11	7.6316 (0.0068)	N4−N11
7.0204 (0.0072)	C5−C8	6.9725 (0.0066)	N5−N8
7.4593 (0.0083)	C7−C10	7.4743 (0.0070)	N7−N10
3.6581 (0.01)	K1−Cl	3.5148 (0.0097)	K1−N1
4.0312 (0.011)	K1−C2	4.0549 (0.011)	K1−N2
4.0346 (0.011)	K1−C3	4.1098 (0.011)	K1−N3
3.5422 (0.010)	K1−C4	3.5849 (0.010)	K1−N4
3.4755 (0.0086)	K1−C5	3.5955 (0.0085)	K1−N5
3.5539 (0.010)	K1−C6	3.6259 (0.010)	K1−N6
3.4828 (0.011)	K1−C7	3.4153 (0.010)	K1−N7
3.5626 (0.0090)	K1−C8	3.6022 (0.0088)	K1−N8
3.5206 (0.011)	K1−C9	3.4750 (0.011)	K1−N9
4.1017 (0.011)	K1−C10	4.1380 (0.010)	K1−N10
4.0751 (0.011)	K1−C11	4.1234 (0.010)	K1−N11
3.7408 (0.010)	K1−C12	3.6092 (0.0099)	K1−N12

(25) Darensbourg, D. J.; Reibenspies, J. H.; Lai, C.-H.; Lee, W.-Z.; Darensbourg, M. Y. *J. Am. Chem. Soc.* **1997**, *119*, 7903.

(26) Williams, D.; Kouvetakis, J.; O'Keefe, M. *Inorg. Chem.* **1998**, *37*, 4617.

(27) Eremenko, I. L.; Pasynskii, A. A.; Abdulaev, A. S.; Aliev, A. S.; Orazsakjatov, B.; Sleptsova, S. A.; Nekhaev, A. I.; Shklover, V. E.; Struchkov, Y. T. *J. Organomet. Chem.* **1989**, *365*, 297.

Table 2. Selected Structural Features (Å) for the $\{Cs[Rh(\mu\text{-}CN)_3]_4Mo_4\}^{3-}$ Core in **2**[a]

9.2631 (0.0011)	Rh1−Mo1A	7.3682 (0.0015)	Rh1−Rh1A
9.2529 (0.0011)	Rh2−Mo3	7.3649 (0.0009)	Rh1−Rh2
9.3379 (0.0015)	Rh3−Mo2	7.4348 (0.0012)	Rh1−Rh3
5.3712 (0.0015)	Rh1−Mo1	7.7300 ((0.0018)	Mo1−Mo1A
5.3643 (0.0010)	Rh1−Rh2	7.7874 (0.0012)	Mo1−Mo2
5.3746 (0.0010)	Rh1−Mo3	7.7033 (0.0010)	Mo1−Mo3
7.2748 (0.015)	N1−N1A	7.0296 (0.018)	C1−C1A
3.6606 (0.0092)	Cs1−C1	3.6731 (0.0075)	Cs1−N1
3.7604 (0.0090)	Cs1−C2	3.8106 (0.0074)	Cs1−N2
3.7307 (0.0081)	Cs1−C3	3.7935 (0.0067)	Cs1−N3
3.8207 (0.0076)	Cs1−C4	3.8567 (0.0067)	Cs1−N4
3.6102 (0.0096)	Cs1−C5	3.6067 (0.0089)	Cs1−N5
3.7661 (0.0088)	Cs1−C6	3.6915 (0.0081)	Cs1−N6
3.6462 (0.011)	Cs1−C7	3.5995 (0.0095)	Cs1−N7

[a] This cage is subject to a crystallographically imposed symmetry plane that contains Cs, Rh2, Rh3, Mo2, Mo3.

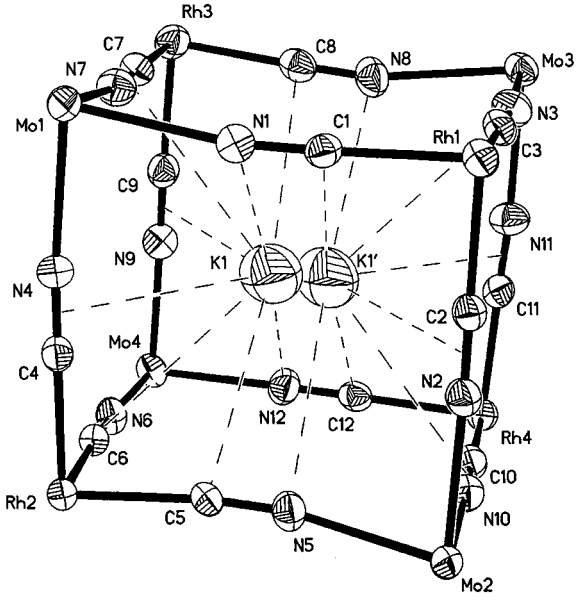

Figure 3. SHELXTL plot of the $\{K[Rh(\mu\text{-}CN)_3]_4[Mo(CO)_3]_4\}^{3-}$ core in **1** (35% probability ellipsoids). Two potassium atoms are distributed over the two sites with almost equal probability (±2.5%).

distance calculated using the Pythagorean theorem is 9.10 Å. The $Mo_4Rh_4(CN)_{12}$ cage is larger than the $M_8(CN)_{12}$ cages for first-row transition metals due to the larger sizes of the second-row metals, which is reflected in a ∼10% increase in both the Rh−C and the Mo−N distances vs analogous cages based on first-row transition metal centers. For example, in Prussian blue the Fe···Fe′ edges are 5.08 Å long.[13]

The only significant difference between **1** and **2** involves the location of the alkali metal cation: in **1** the K^+ is situated in one of two off-center positions, with almost equal populations (Figure 3). In **2**, the Cs^+ is located at the center of the cage (Figure 4). Thus, **1** has idealized C_{2v} symmetry whereas **2** has idealized T_d symmetry. The degree of centering of the Cs^+ in **2** is indicated by the fact that the Mo−Cs−Mo and Rh−Cs−Rh angles are 109 ± 1°. The Cs···C and Cs···N distances range from 3.6 to 3.85 Å; the average of the Cs−C and Cs−N distances are the same at 3.71 Å. In **1**, the K···C/N distances span a broader range of 3.475−4.12 Å. These K···C/N contacts fall into four relatively distinct sets, as dictated by the symmetry and as is obvious from visual inspection. At one end of the box, the K^+ is bound in a pocket of 12 C/N atoms with K··· C/N distances of 3.4153(10)−3.6092(99) Å.

In both **1** and **2**, nine molecules of MeCN and one molecule of Et_2O are located in the asymmetric unit. The CH_3 groups of

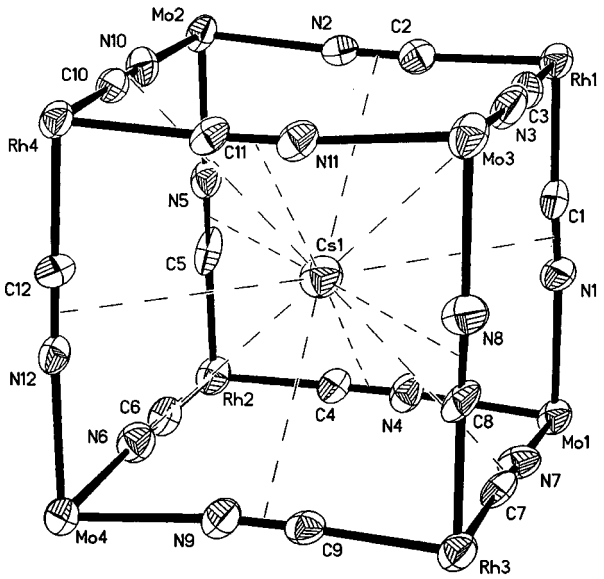

Figure 4. SHELXTL plot of the $\{Cs[Rh(\mu\text{-}CN)_3]_4[Mo(CO)_3]_4\}^{3-}$ core in **2** (35% probability ellipsoids).

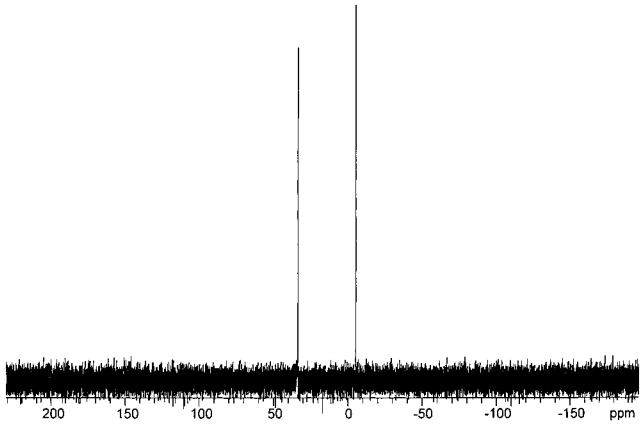

Figure 5. 65.5 MHz ^{133}Cs NMR spectra of a MeCN solution of $\{Cs[Cp^*Rh(\mu\text{-}CN)_3]_4[Mo(CO)_3]_4\}^{3-}$ in the presence of added CsOTf.

six molecules of MeCN are situated near the square $Mo_2Rh_2C_4N_4$ faces of the box, as is also seen in $\{[CpCo(\mu\text{-}CN)_3]_4[Cp^*Rh]_4\}(PF_6)_4$.[20]

^{133}Cs NMR Measurements. The binding of the alkali metal at the cage interior was examined by ^{133}Cs NMR studies on MeCN solutions of **2**.[28] ^{133}Cs has the following nuclear magnetic resonance characteristics: 100% natural abundance with a resonant frequency at 13.116 MHz (vs 100 MHz for ^1H). The nucleus is quadrupolar ($I = 7/2$) but with only a small quadrupole moment of -3×10^{25} m^2, comparable to that for ^2H but opposite in sign.[29] MeCN solutions of CsOTf display a sharp signal at δ 32. In contrast, MeCN solutions of **2** show a single resonance at δ −5.0. The addition of free CsOTf to a solution of **2** gave a new peak at the free Cs^+ position (δ 32), thus verifying slow exchange between interior and exterior Cs^+ centers (Figure 5). The line width at half-height for free Cs^+ (δ 32) is 7.1 Hz, while for Cs^+ in the box, the line width is 4.0 Hz for natural abundance species. For samples of **2** prepared from ^{13}CN, the ^{133}Cs line width is 6.6 Hz, an increase in the line width attributed to unresolved $J(^{133}Cs,^{13}C)$ coupling.

(28) Mei, E.; Popov, A. I.; Dye, J. L. *J. Am. Chem. Soc.* **1977**, *99*, 6532.
(29) Brevard, C.; Granger, P. *Handbook of High-Resolution NMR*; Wiley: New York, 1981.

The addition of 2× excess $KB(C_6H_4\text{-}4\text{-}Cl)_4$ to a solution of **2** resulted in no change in the spectrum, indicative of either the preferential binding of Cs^+ vs K^+ or the slow approach to equilibrium. In a separate experiment, 1 equiv CsOTf was added to a solution consisting of **1** and 9 equiv of $KB(C_6H_4\text{-}4\text{-}Cl)_4$. Within the time needed to acquire the spectrum (∼1 h), the only ^{133}Cs NMR resonance observed was for **2** at $-\delta$ 5.0. This experiment demonstrates two facts: the cyanometalate cage prefers to bind Cs^+ vs K^+, and alkali metal exchange is facile. The relative binding affinity for Cs^+ vs K^+ can be expressed as eq 4

$$K_{eq} = [\mathbf{2}][K^+]/[\mathbf{1}][Cs^+] \quad (4)$$

We estimate the detection limit of the NMR measurement to be 5%, leading to the assumption that at least 95% of **1** was converted to **2**. In the presence of an initial 9-fold excess of K^+, eq 4 can be expressed as eq 5, recognizing that $[\mathbf{1}]_o = [Cs^+]_o = (1/9)[K^+]_o$,

$$K_{eq} \geq (0.95[\mathbf{1}]_o)(9.95[\mathbf{1}]_o)/(0.05[\mathbf{1}]_o)^2 \quad (5)$$

which can be solved knowing that $[\mathbf{1}]_o = 0.00347$ M, which gives a lower limit for K_{eq} of 3780.

Discussion

The ability of the cyano ligands to serve as a bridging ligand has long been known and many multimetallic complexes have been prepared by capitalizing on this property.[30] Molecular squares with $M_4(\mu\text{-}CN)_4$ cores are well precedented, and more complex structures are known, e.g., $Cr[CNCr(CO)_5]_6^{3-}$ and $Cr[CNNi(amine)_5]_6^{3+}$.[31,32] The preparation of *cages* based on CN bridges is an ancient art, as demonstrated by the long tradition of Prussian blue and its many analogues.[33] The innovation described in this and related papers is the preparation of *molecular* cages based on M−CN−M′ linkages.[20,21,34] Previously we prepared cationic cyanometalate cages by the reaction of Cp^*M^{2+} and $Cp^*M(CN)_3^-$ species. In this work we found that related anionic cages could only be obtained in the presence of alkali metal cations. The stability conferred by the alkali metal is unusual because, in contrast to traditional complexes, the interaction between the alkali metal and the surrounding polycyanide framework is ionic.

Competition experiments show that the cage has a higher affinity for Cs^+ than K^+ (eq 6). The structures of **1** and **2**

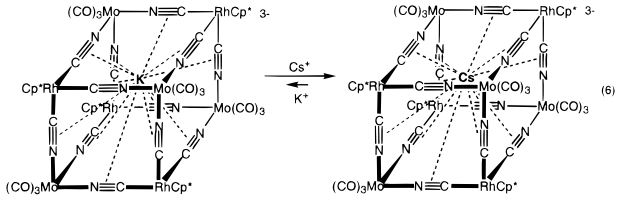

indicate that the preferential binding of larger alkali metal cations by solid cyanometalates is due to a better fit of Cs^+ in the $M_8(CN)_{12}$ cage (Figure 6). The poorer fit of K^+ in the cage is indicated by the fact that it is disordered over two sites. The rigidity of the $M_8(CN)_{12}$ framework prevents this inorganic ligand from collapsing around the smaller K^+, thus ensuring ion selectivity. The rigidity of the $Mo_4Rh_4(CN)_{12}$ cage is indicated by the very similar structures of the cages in **1** and **2**.

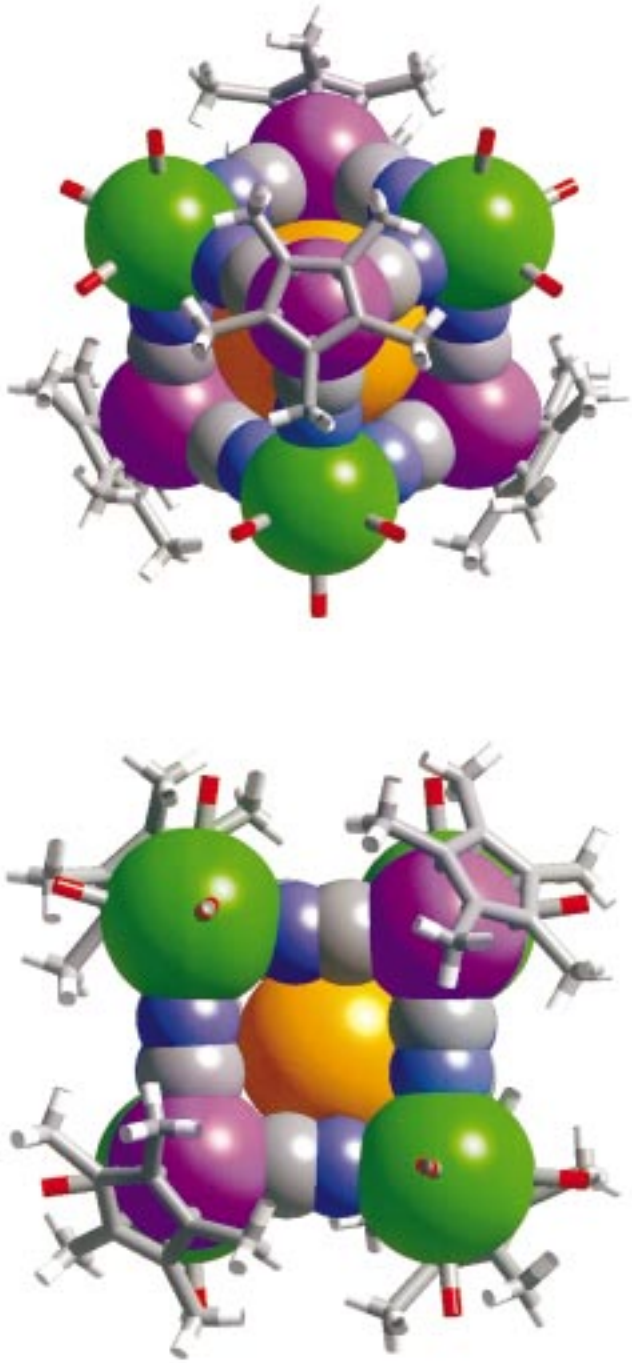

Figure 6. Structures of $\{Cs[Cp^*Rh(\mu\text{-}CN)_3]_4[Mo(CO)_3]_4\}^{3-}$ (top) and $\{K[Cp^*Rh(\mu\text{-}CN)_3]_4[Mo(CO)_3]_4\}^{3-}$ (bottom) using the following radii: $r_C = 0.77$, $r_{Cs} = 2.40$, $r_K = 2.06$, $r_{Mo} = 1.31$, $r_N = 0.74$, $r_{Rh} = 1.21$ Å.

Although the systems discussed in this paper are not practical, our results demonstrate promising host−guest behavior of *molecular* cyanometalate cages. The mechanism of alkali metal exchange is of continuing interest. At present, it remains unclear if the box disassembles prior to alkali metal exchange; alternatively, the entering alkali metal could associate with one face, followed by an interchange process. Further experiments are planned to explore this point.

(30) Vahrenkamp, H.; Geiss, A.; Richardson, G. N. *J. Chem. Soc., Dalton Trans.* **1997**, 3643.
(31) Fritz, M.; Rieger, D.; Bär, E.; Beck, G.; Fuchs, J.; Holzmann, G.; Fehlhammer, W. P. *Inorg. Chim. Acta* **1992**, *198*, 513.
(32) Mallah, T.; Auberger, C.; Verdaguer, M.; Veillet, P. *J. Chem. Soc., Chem. Commun.* **1996**, 61.
(33) Macquer, P. J. *Acad. R. Science (France)* **1752**, *2*, 87.
(34) Contakes, S. E.; Klausmeyer, K. K.; Milberg, R. M.; Wilson, S. R.; Rauchfuss, T. B. *Organometallics* **1998**, *19*, 3633.

Experimental Section

General Protocols. Most operations were conducted in an inert atmosphere box. The following reagents were purchased from Aldrich or were prepared according to literature methods: $K^{13}CN$, (η^6-$C_6H_3Me_3$)$Mo(CO)_3$,[35] $[Cp^*RhCl_2]_2$, CsOTf (gift of S. Holmes and G. S. Girolami), KOTf, and $KB(C_6H_4Cl)_4$.

Electrospray mass spectra were recorded on a Quattro quadrupole−hexapole−quadrupole (QHQ) mass spectrometer. ^{133}Cs NMR spectra were recorded on a Varian Unity 500 wide bore spectrometer equipped with a broad-band probe. ^{133}Cs chemical shifts are referenced to 0.05 M aqueous CsI (δ 0). ^{1}H and ^{13}C NMR spectra were obtained with a Varian Unity 500 instrument. EDX measurements were performed on a Zeiss DSM 960 scanning electron microscope.

Synthesis of $(Et_4N)[Cp^*Rh(CN)_3]$. A slurry of 0.30 g (0.485 mmol) of $[Cp^*RhCl_2]_2$ in 50 mL of H_2O was treated with 0.329 g (1.94 mmol) of $AgNO_3$. After 40 min, the yellow solution was separated from the AgCl by filtration through Celite. The filtered solution was treated with 0.284 g (4.5 equiv/Rh, 4.36 mmol) of KCN. After 12 h, the colorless solution was treated with 0.161 g (0.970 mmol) of Et_4NCl. The solvent was evaporated, leaving a pale yellow solid. The yellow solid was extracted into 30 mL of CH_2Cl_2 which was filtered to remove KCl, KCN, and KNO_3. The product, $(Et_4N)[Cp^*Rh(CN)_3]\cdot H_2O$, precipitated upon the addition of hexane. Yield 0.401 g (93%). ^{1}H NMR ($CDCl_3$) δ 3.40 (q, 8H), 1.93 (s, 15H), and 1.36 (t, 12H). $^{13}C\{^1H\}$ NMR ($CDCl_3$) δ 129.1, 128.7 (*C*N J_{C-Rh} = 51 Hz), 100.61, 100.57 (Me_5C_5 J_{C-Rh} = 4.6 Hz), 52.7 ($(CH_3CH_2)_4N$), 9.9 ($(CH_3)_5C_5$) 7.7 ($(CH_3CH_2)_4N$). FAB MS *m*/*z* 316.0 (M^-). IR ν_{CN} (KBr) 2110, 2122 cm^{-1}. Anal. Calcd for $C_{21}H_{35}N_4Rh\cdot H_2O$ C, 54.31; H, 8.03; N, 12.06. Found C, 53.96; H, 8.20; N, 11.97.

$(Et_4N)_3\{M^+[Cp^*Rh(\mu\text{-}CN)_3]_4[Mo(CO)_3]_4\}$. In air, 0.050 g (0.168 mmol) of ($C_6H_3Me_3$)$Mo(CO)_3$, 0.075 g (0.168 mmol) of $(Et_4N)[Cp^*Rh(CN)_3]$, and 0.021 g (0.042 mmol) of $KB(C_6H_4Cl)_4$ (for **1**) or 0.011 g (0.042 mmol) of CsOTf (for **2**) were placed in a 50-mL round-bottom flask, which was then transferred into a glovebox. The mixture was dissolved in 10 mL of MeCN. After 2 h, the color had darkened from a pale yellow to orange. The solution was diluted with 35 mL of Et_2O, resulting in the precipitation of an orange solid.

For **1**: Yield 0.065 g (64% based on $(Et_4N)[Cp^*Rh(CN)_3]$). IR ν_{CN} = 2147, ν_{CO} = 1893(s) and 1768(vs) cm^{-1}. ^{1}H NMR (CD_3CN) δ 3.15 (q, 24H, $N(CH_2CH_3)_4$), 1.994 (s, 60H, Cp*), 1.19 (t, 36H, $N(CH_2CH_3)_4$). ^{13}C NMR (CD_3CN) δ 128.3 (d, fwhh = 2.8 Hz, CN, J_{C-Rh} = 51 Hz). ESI MS 1077.8 ($\{(NEt_4)_2K[Cp^*Rh(CN)_3]_4[Mo(CO)_3]_4\}^-$), 496 ($[Cp^*Rh(CN)_3][Mo(CO)_3]^-$). EDX analysis (atom % relative to KMo_4Rh_4), theory K, 11.11; Mo, 44.44; Rh, 44.44. Found K, 10; Mo, 45; Rh, 44.

For **2**: Yield 0.077 g (73% based on $(Et_4N)[Cp^*Rh(CN)_3]$). IR ν_{CN} = 2147 cm^{-1}, ν_{CO} = 1893(s), 1768(vs) cm^{-1}. ^{1}H NMR (CD_3CN) δ 3.15 (q, 24H, $N(CH_2CH_3)_4$), 1.988 (s, 60H, Cp*), 1.19 (t, 36H, $N(CH_2CH_3)_4$). ^{13}C NMR (CD_3CN) δ 129.1 (d, fwhh = 9.3 Hz, *C*N, J_{C-Rh} = 51 Hz). ^{133}Cs NMR (vs CsI in D_2O) $-\delta$ 5. ESI MS 705.8 ($\{Cs[Cp^*Rh(CN)_3]_4[Mo(CO)_3]_4\}^{3-}$), 496 ($\{[Cp^*Rh(CN)_3][Mo(CO)_3]\}^-$). Anal. Calcd for $(Et_4N)_3\{Cs[Mo(CO)_3]_4[Cp^*Rh(CN)_3]_4\}$ C, 42.14; H, 4.82; N, 8.38. Found C, 42.54; H, 4.81; N, 8.07. EDX analysis (atom % relative to $CsMo_4Rh_4$), theory Cs, 11.11; Mo, 44.44; Rh, 44.44. Found Cs, 10; Mo, 45; Rh, 44.

For the NMR tube experiments, 0.010 g (0.033 mmol) of (η^6-$C_6H_3Me_3$)$Mo(CO)_3$, 0.015 g (0.033 mmol) of $(Et_4N)[Cp^*Rh(CN)_3]$, and 0.002 g (0.0075 mmol) of CsOTf were dissolved in 1 mL of MeCN-d_3. The solution was mixed for 5 min and then transferred to an NMR tube for analysis.

Crystallographic Analysis of 1. The data crystal, an orange block was mounted using oil (Paratone-N Exxon) to a thin glass fiber with the (1 0 −1) scattering planes roughly normal to the spindle axis. Data were collected on a Siemens Smart CCD detector using 0.25°/s ω scan width and 20 s scan time.[36] Of 145 519 reflections collected for θ ranging from 1.38 to 25.08°, 23502 were independent with R_{int} = 0.0683, after SADABS absorption correction.[36] Details of the crystal data and refinement are given in Table 3.

The structure was solved by direct methods (SHELXS[36]), which showed the position of all of the atoms of the box and one Et_4N^+. Subsequent least-squares refinements (SHELXL 97-2[37]) located the positions of the remaining atoms in the electron difference map. All non-H atoms were refined anisotropically except for disordered solvent molecules and one acetonitrile. Final refinement cycles were performed using SHELXH 97-2[36] due to the large number of parameters. Four reflections were omitted in the final structure calculation, (1 1 2), (0 2 2), (0 2 1), and (0 0 4); these reflections were truncated by the beamstop. The largest residual peak (2.008 e$^-$/Å^3) was located at 0.85 Å from Rh2.

The K^+ ion is disordered over two positions parallel to the C1−N1, C5−N5, C8−N8, and C12−N12 cyanide ligands. The site occupancy was restrained to sum to unity and refined to a value of nearly 50% (51.4 and 48.6 for the other) per position. Equivalent U's of the K^+ ion were restrained to be similar within 0.005 due to high correlation.

The Cp* rings were refined as variable metric rigid groups. The Cp* rings bound to Rh3 and Rh4 were found to be disordered. For each, two orientations were found; the Cp* bound to Rh3 consists of a 64/36 disorder, and the Cp* bound to Rh4 consists of an 83/17 disorder. Carbon atoms of each ring were restrained to have similar U's within 0.01.

Only one of the Et_4N^+ counterions was ordered; for this cation, no restraints were imposed. The other two Et_4N^+ cations were disordered over two positions, which refined to occupancies of 68/32 for N14 and 73/27 for N15. For the disordered cations, the N−C distances were restrained to 1.51(1) Å and the C−C distances were restrained to 1.53(1) Å. The 1−3 N−C distances were restrained to 2.52(1) Å. All non-H atoms of the counterions were refined anisotropically. For the two disordered cations, the anisotropic displacement parameters were restrained to have similar U's within 0.01.

Nine molecules of acetonitrile are present in the asymmetric unit; six are associated with the faces of the box. Disorder was found for two of acetonitrile molecules (N20 and N24); the N20 acetonitrile is disordered over two positions of occupancy of 77/23. The N24 acetonitrile is disordered over three positions with occupancies of 31, 31, and 38%. Equivalent atoms of the individual disordered molecules of acetonitrile were restrained to have the same isotropic displacement parameters and refined as rigid groups. The N22 acetonitrile was refined isotropically as a rigid group.

One molecule of diethyl ether is disordered over two positions of 58 and 42% occupancy. The intermolecular distances were restrained to 1.42(1) Å for the O−C bonds and 1.53(1) Å for the C−C bonds. The 1−3 O−C distances were restrained to 2.319(1) Å. The isotropic displacement parameters of the ether atoms were restrained to be the same.

Crystallographic Analysis of 2. The data crystal, an orange needle, was mounted using a CryoLoop fiber with the (1 0 −1) scattering planes roughly normal to the spindle axis. The rapid desolvation of these crystals severely inhibited crystal selection. Data were also collected on a Siemens Smart CCD detector using 0.25°/s ω scan width and 20 s scan time.[36] Of 73 903 reflections collected for θ ranging from 1.55 to 25.02°, 12 454 were independent with R_{int} = 0.1144 after SADABS absorption correction.[36] Details of the crystal data and refinement are given in Table 3.

The structure was solved by direct methods (SHELXS[36]), which showed the position of one-half of the framework atoms of the box and one-half of the ordered Et_4N^+. Subsequent least-squares refinements (SHELXL 97-2[37]) located the positions of the remaining atoms in the electron difference map. The structure features a mirror plane passing through the box on a diagonal containing the metals Cs1, Rh2, Rh3, Mo2, and Mo3. Three reflections were omitted in the final structure calculation, (0 2 2), (0 2 1), and (1 1 1); these reflections were truncated by the beamstop. The largest residual peak was 1.87 e$^-$/Å^3 at 0.92 Å from Rh2.

(35) Girolami, G. S.; Rauchfuss, T. B.; Angelici, R. J. *Synthesis and Technique in Inorganic Chemistry*; University Science Books: Mill Valley, CA, 1999.

(36) Sheldrick, G. M., SAINT v5 and SHELXTL v5, Bruker AXS, Madison WI, 1998.

(37) Sheldrick, G. M., SHELXL-97, University of Göttingen, 1997.

Table 3. Crystal Data and Structure Refinement for $(Et_4N)_3\{M[Cp^*Rh(CN)_3]_4[Mo(CO)_3]_4\}\cdot(CH_3CN)_9\cdot Et_2O$ for M = K, (**1**), Cs (**2**)

empirical formula	$C_{110}H_{157}KMo_4N_{24}O_{13}Rh_4$	$C_{110}H_{157}CsMo_4N_{24}O_{13}Rh_4$
formula weight	2858.10	2951.91
temperature	198(2) K	198(2) K
wavelength	0.710 73 Å	0.710 73 Å
crystal system	orthorhombic	orthorhombic
space group	*Pbca*	*Cmca*
unit cell dimensions from 8192 reflns with $4 = \theta = 28$		
a (Å)	17.8255(2)	17.7795(5)
b (Å)	30.4826(4)	30.585(2)
c (Å)	50.0321(7)	50.1116(4)
α (deg)	90	90
β (deg)	90	90
γ (deg)	90	90
V (Å^3)	27185.8(6)	27250(2)
Z	8	8
density (calculated)	1.397 mg/m^3	1.439 mg/m^3
absorption coefficient	0.920 mm^{-1}	1.151 mm^{-1}
crystal size	0.58 × 0.48 × 0.20 mm	3.0 × 0.14 × 0.14 mm
theta range for data collection	1.38−25.08°	1.55−25.02°
index ranges	$-20 \le h \le 20$	$-19 \le h \le 21$
	$-36 \le k \le 35$	$-36 \le k \le 35$
	$-59 \le l \le 59$	$-59 \le l \le 59$
collection method	0.25° *ω* scans for 0.333 min/scan	0.25° *ω* scans for 0.333 min/scan
reflections collected	145 519 [$R_{int} = 0.0683$]	73 903 [$R_{int} = 0.1144$]
independent reflections	23 502 [15 103 obsd, $I > 4\sigma(I)$]	12 454 [7349 obsd, $I > 4\sigma(I)$]
absorption correction	SADABS	SADABS
max. and min. transmission	0.978 and 0.641	0.978 and 0.248
refinement (shift/err = −0.001)	full-matrix least-squares on F^2	full-matrix least-squares on F^2
data/restraints/parameters	23502/642/1588	12454/257/768
goodness-of-fit[a] on F^2	1.256	1.120
final *R* indices (obsd data)[b,c]	R1 = 0.0511, wR2 = 0.1020	R1 = 0.0716, wR2 = 0.1789
R indices (all data)*	R1 = 0.0857, wR2 = 0.1092	R1 = 0.1215, wR2 = 0.1965
largest diff. peak and hole	1.540 and −0.575 e$^-$/Å^{-3}	1.865 and −1.031 e$^-$/Å^{-3}

[a] The weighting of the structures was adjusted to provide a GOF of approximately 1.00 at a data cutoff of 3σ. This was 0.90 Å resolution for **1** and 1.05 Å resolution for **2**. [b] $R1 = \sum||F_o| - |F_c||/\sum|F_o|$. $wR2 = \sum[w(F_o2 - F_c2)^2/\sum w(F_o2)^2]^{1/2}$. [c] $w = 1/[\sigma^2(F_o^2) + (0.0100P)^2]$, where $P = (F_o^2 + 2F_c^2)/3$.

All Cp* ligands were refined as fixed groups. The Cp* ligands for Rh2 and Rh3 were modeled as a 50/50 disorder about the mirror plane passing through the box. Carbon atoms of each ring were restrained to have similar U's within 0.01.

Nine molecules of acetonitrile are present in the symmetric unit, and six are associated with the faces of the box. Those molecules with N11, N12, N13, and N14 were located near the faces of the cage, while two other such molecules were generated by symmetry, all of these were refined anisotropically. Those molecules of acetonitrile containing N13 and N14 were disordered and modeled at 50% site occupancy. The N15 acetonitrile was refined at 50% site occupancy due to symmetry; because of high thermal parameters, these atoms were refined isotropically. The N16 acetonitrile was well behaved and refined anisotropically at 50% site occupancy due to a symmetry. The last acetonitrile is disordered over several positions; two major positions (N17 and N18) were refined isotropically at 25% site occupancy with the remaining 50% being generated by symmetry.

Only one of the Et_4N^+ counterions was ordered; for this cation no restraints were placed on the model. The other two cations were grossly disordered. For these, the N−C distances were restrained to 1.51(1) Å, and the C−C distances were restrained to 1.53(1) Å. The 1−3 N−C distances were restrained to 2.52(1) Å. For the disordered Et_4N^+ ions only the N atoms were refined anisotropically.

One molecule of diethyl ether is present, the intermolecular distances were restrained to 1.42(1) Å for the O−C bonds and 1.53(1) Å for the C−C bonds. The 1−3 O−C distances were restrained to 2.319(1) Å. The isotropic displacement parameters of the ether atoms were restrained to be the same.

Acknowledgment. This research was supported by the Department of Energy under contract DEFG02-90ER14146. Electron microscopic characterizations were performed at the Center for Microanalysis of Materials, supported by the DOE contract DEFG02-96ER45439. We thank Stephen Contakes for valuable discussions.

Supporting Information Available: Crystallographic data for **1** and **2** (PDF). This material is available free of charge via the Internet at http://pubs.acs.org.

JA982347W